Ignition and Flame Propagation in Dilute Polydisperse Sprays; Importance of d_{32} and d_{20}

Suresh K. Aggarwal*
The University of Illinois at Chicago, Chicago, Illinois

Suitability of the Sauter mean diameter and the surface-area mean diameter for representing the ignition and combustor behavior of polydisperse sprays is examined. Initial size distributions considered are the Nukiyama-Tanasawa distribution and a bidisperse spray. Two physical situations are analyzed. In the first, the ignition characteristics of a polydisperse spray in the viscinity of a hot wall are studied. In the second, the flame propagation through a mixture of air and polydisperse spray in a constant-volume combustor is investigated. For both situations, the relevant two-phase equations are solved by a hybrid Eulerian-Lagrangian numerical method. The results indicate that the ignition behavior of polydisperse sprays is best represented by the surface-area mean diameter, whereas the flame propagation characteristics are best correlated by the Sauter mean diameter. These correlations are observed over a wide range of initial droplet size, size distribution, fuel volatility, and overall equivalence ratio, which is typical in practical combustion systems.

Nomenclature

d = droplet spacing
d_{20} = surface-area mean diameter
d_{32} = Sauter mean diameter
E_r = overall equivalence ratio based on the total fuel mass and air mass
L = tube length
m_f = liquid fuel mass initially present in the tube
M = mass [see Eqs. (6) and (8)]
n = number of droplets per unit area [Eq. (10)]
x = droplet diameter
X = spatial location in the figures
y = normalized mean diameter [Eqs. (7) and (8)]
Y_F = fuel vapor mass fraction
Y_o = oxygen mass fraction
Δt = temporal step size
ΔX = spatial step size
ΔM_k = fraction of liquid mass in size group k
ρ_ℓ = liquid density

Subscript

k = droplet size group

Introduction

THE fuel sprays in most combustion applications are polydisperse in nature. One problem that has often confounded the modeling community is the availability of initial size distribution for a given spray. Moreover, the numerical efforts involved in solving polydisperse sprays with any realistic size distribution could be enormous. These problems are usually circumvented by employing the concept of an "equivalent" monodisperse spray with a suitable mean droplet size. The Sauter mean diameter (SMD) has most frequently been cited as the suitable mean size. The expectation is that the equivalent spray adequately represents the behavior of the corresponding polydisperse spray, at least in a global sense. The approach remains open to question for two reasons. First, there is no substantial evidence that a monodisperse spray with a suitably defined mean size can indeed simulate the characteristics of the polydisperse spray. Second, it is not well established that the Sauter mean diameter is always the most appropriate mean diameter for the equivalent monodisperse spray as the existing studies[1-3] provide conflicting results. For example, Dickinson and Marshall[1] concluded that for diffusion-controlled vaporization, no mean diameter can adequately represent the vaporization characteristics of polydisperse sprays. Alkidas[2] conducted an analytical study for steady-state vaporization as given by d^2 law[4] and concluded that the Sauter mean diameter best correlates the overall vaporization behavior of sprays of different initial size distributions for both diffusion-controlled and radiation-controlled vaporization. A recent study by Aggarwal and Sirignano,[3] however, indicated that the ignition characteristics of polydisperse sprays are best correlated by surface-area mean diameter and not by SMD.

The present investigation is aimed at examining these issues. The problem of ignition and unsteady flame propagation in polydisperse sprays is numerically solved. The Nukiyama-Tanasawa distribution[5] and a bidisperse distribution are considered. The ignition as well as the flame propagation characteristics of polydisperse sprays are compared, both locally and globally, with their corresponding equivalent monodisperse sprays of SMD and surface-area mean diameter. From the comparisons, conclusions are made regarding the mean diameter that best correlates the behavior of polydisperse sprays.

The present study is important because none of the earlier works[1-3] has conducted a systematic comparison, based on a detailed numerical study, of polydisperse and equivalent monodisperse sprays. Moreover, none of them has compared the combustion characteristics of these sprays, which is important because the combustion behavior of polydisperse sprays may be qualitatively different from those of equivalent monodisperse sprays. For example, the small droplets in the presence of large droplets can significantly alter the burning mechanism. The large droplets may burn in a flame that is established by smaller droplets.

The present paper may be considered an extension of an earlier study[3] to the extent that it essentially employs the same physical model. The earlier work, however, considered only the ignition behavior of polydisperse sprays with initial size distribution idealized by a bidisperse distribution. In this

Presented as Paper 86-1525 at the AIAA/SAE/ASME/ASEE 22nd Joint Propulsion Conference, Huntsville, AL, June 16-18, 1986; received Feb. 24, 1987; revision received June 3, 1987.

*Assistant Professor, Department of Mechanical Engineering. Member AIAA.

paper, the ignition as well as the combustion behavior are investigated. In addition, more realistic initial size distributions, such as that of Nukiyama–Tanasawa,[5] are considered. To the author's knowledge, none of the previous studies has compared the combustion characteristics of a polydisperse spray with its equivalent monodisperse sprays.

The physical model and the governing equations are described in the next section, followed by a discussion of different droplet size distributions. Then, the results are discussed. Finally, the conclusions regarding the most appropriate mean diameter for representing the polydisperse sprays are presented.

Physical Model and Governing Equations

The physical model used in the present study has been discussed in earlier papers.[3,6,7] Thus, most of the details will be avoided here. Essentially, a polydisperse spray-air mixture that is initially quiescent and contained in a tube is considered. The left end of the tube is closed and an isothermal boundary condition is employed there. It is also used as an ignition source to initiate the flame propagation into the mixture. The right end is also closed but an adiabatic boundary condition is used there. The governing equations used to predict the gas-phase and liquid-phase properties are written in a hybrid Eulerian–Lagrangian system. The gas phase is treated in the Eulerian frame of reference, whereas the Lagrangian approach is used for the liquid phase. Other notable features of the mathematical model are that the transient heat transport inside the droplets is considered via an unsteady spherically symmetric model, and the fuel-oxidation model is global, given by a one-reaction scheme with nonunity exponents of fuel and oxygen concentrations. The reasons for this particular choice were discussed in earlier studies.[3,6] The chemical kinetics parameters are essentially the same as those used in Ref. 6. The only difference is due to the values of pre-exponential constants for normal hexane and normal decane fuels. The values in the present case are 3.9×10^{11} and 2.6×10^{11} cm^3 mole^{-1} s^{-1}, respectively, as compared to 5.7×10^{11} and 3.8×10^{11} in Ref. 6. The lower values have been found to better correlate with the results of a more detailed kinetics scheme.[8]

An explicit finite-difference scheme is employed to solve the gas-phase equations, whereas a second-order Runge–Kutta integration is used to solve the liquid-phase equations. The details of the numerical procedure can also be found in earlier studies.[3,4] Essentially, the temporal evaluation of ignition is followed by solving the two-phase equations. The occurrence of ignition is defined by the zero heat flux condition at the left end. This provides a sufficient condition for ignition and for the generation of a self-supporting flame. It also defines the ignition delay time. The propagation is then followed by computing the profiles of various gas- and liquid-phase properties at different times. The flame propagation behavior is studied for different initial size distributions that are discussed next.

Initial Droplet Size Distribution

The droplet size distribution in sprays produced in most applications is generally correlated by the expression[2,9]

$$\frac{dn}{n} = ax^{\alpha}\exp(bx^{\beta})dx \tag{1}$$

where dn/n represents the fraction of the number of droplets with diameter between $x + dx$. The constants α and β are to be determined experimentally. The coefficient a is determined from the total number of droplets, i.e., from the condition that the integration of Eq. (1) should be unity. The coefficient b can be expressed in terms of some suitable mean diameter defined as

$$\bar{x}_{ij} = \left\{\int_0^\infty x^i dn \Big/ \int_0^\infty x^j dn\right\}^{\frac{1}{i-j}} \tag{2}$$

For example, with the Sauter mean diameter (SMD)

$$x_{32} = \int_0^\infty x^3 dn \Big/ \int_0^\infty x^2 dn \tag{3}$$

and after the substitution of Eq. (1)

$$x_{32} = \left(\frac{1}{b}\right)^{1/\beta}\Gamma\left(\frac{\alpha+4}{\beta}\right)\Gamma\left(\frac{\alpha+3}{\beta}\right) \tag{4}$$

where Γ is the Gamma function defined as

$$\Gamma(k) = \int_0^\infty x^{k-1}\exp(-x)dx \tag{5}$$

The selection of x_{32} completes the specification of droplet size distribution for given values of α and β. The droplet mass distribution is then easily obtained from the size distribution. For spherical single-component fuel droplets, the mass of droplets of diameters between x and $x + dx$ is

$$dM = (\Pi/6)\,\rho_\ell x^3 dn \tag{6}$$

Note that the notation of Ref. 2 is adopted here. Also, note that different types of size and mass distributions can be obtained by changing α and β. The most cited distributions are the Rosin–Rammler distribution,[10,11] the Nukiyama-Tanasawa distribution,[5] and the Hiroyasu-Kadota distribution.[12] In the present study, the Nukiyama-Tanasawa distribution ($\alpha=2$, $\beta=1$) is employed. Then, the following expression can be obtained for the droplet size and mass distributions:

$$\frac{dn}{n} = 6.25y^2\exp(-5y)dy \tag{7}$$

$$\frac{dM}{M} = \frac{5^5}{24}y^5\exp[-5y]dy \tag{8}$$

where y is the droplet diameter normalized by the Sauter mean diameter. The variation of $(dn/n)/dy$ and $(dM/M)/dy$ with y is shown in Fig. 1. We should note that numerical computations require that the continuous mass distribution be approximated by discrete mass distribution. In the present study, it is assumed that four size intervals with $dy=0.6$, shown crosshatched in Fig. 1, can represent the continuous distribution reasonably well. Then, the total mass ΔM and the mean normalized droplet diameter $\bar{y}$ for each size interval can be easily obtained. These are given in Table 1, where $\bar{y}$ corresponds to the location of average height in each crosshatched area. Also note that the discretization of continuous mass distribution modifies curve A_2 somewhat such that $A_2=0$ at $y=2.4$ (see Fig. 1). The area outside the modified curve is included in the range of $\bar{y}$ between 1.8–2.4. Then, for a given SMD, the droplet diameters for the four discrete mass distributions can be obtained. For SMD = 50 μm, the values are given in Table 1.

The procedure to specify the initial spray properties is as follows. The total liquid fuel mass (m_f) that is initially present in the enclosed tube can be obtained from the given overall equivalence ratio, gas properties, and initial fuel vapor mass fraction, if any [see Eq. (1) of Ref. 3]. Then, ΔM, given in

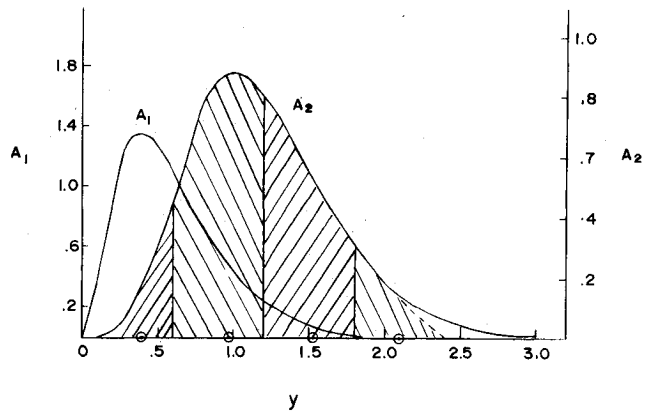

Fig. 1 The Nukiyama-Tanasawa size (A_1) and mass (A_2) distributions.

Table 1 Discretized Nukiyama-Tanasawa distribution

y range $(y_1 - y_2)$	$\Delta M = \int_{y_1}^{y_2} \frac{dM}{M}$	y	x (with SMD = 50 μm)
0–0.6	0.08	0.40	20 μm
0.6–1.2	0.48	0.96	48
1.2–1.8	0.33	1.52	76
1.8–2.4	0.11	2.10	105

Table 1, yields the liquid fuel mass for each size group k, written as

$$m_k = \Delta M_k m_f, \qquad k = 1, 2, 3, 4 \tag{9}$$

The quantity m_k can also be expressed as

$$m_k = (\pi/6)\, L \rho_l n_k x_k^3 / d_k \tag{10}$$

If we assume that d_k varies inversely with the square root of n_k, i.e., the droplet spacing is isotropic, we can obtain n_k and d_k from Eq. (10) as x is known from Table 1. This completes the specification of the initial spray properties for the Nukiyama–Tanasawa distribution. Also, note that for the Hiroyasa-Kadota distribution,[12] the curve A_2 (see Fig. 1) will be flatter with relatively more mass in higher droplet sizes. However, the results presented here are not expected to be significantly different for that distribution.

Another size distribution that is considered in this paper corresponds to a bidisperse spray with mass equally distributed in two droplet sizes, i.e., $\Delta M_k = 0.5$ with $k = 1$ and 2. Obviously, this distribution does not correspond to any of the distributions discussed so far. The purpose here essentially is to examine the flame propagation results for a distinctly different distribution and to show that the major conclusions are not size-distribution dependent.

Results and Discussion

The general spray ignition and flame characteristics have been discussed in earlier papers.[3–6] The results presented here will focus on whether the ignition and combustion behavior of polydisperse sprays can be represented by equivalent monodisperse sprays. First, the flame propagation behavior is discussed. Following that, the ignition characteristics are discussed.

Results of Spray Flame Propagation

The flame characteristics of several polydisperse sprays have been computed and compared with those of the d_{32} and d_{20} monodisperse sprays. In the following discussion, a d_{32} monodisperse spray corresponds to the equivalent monodisperse spray of diameter equal to the Sauter mean diameter. Similarly, a d_{20} monodisperse spray is one in which the droplet diameter is equal to the surface-area mean diameter of the polydisperse spray. Since this study considers flame propagation in a constant volume combustor, a convenient method of comparison on a global basis is to plot the combustor pressure vs time. As shown in the Appendix, the pressure vs time plot provides a good measure for the speed of flame propagation in the constant volume case. Although this global comparison has been used here in most situations, in some cases a local comparison is also given.

The first set of calculations was directed at finding the appropriate grid size for the present results. The values of the time step and grid size that yield reasonably grid-independent solutions are found to be 5 μs and 0.025 cm, respectively. The effect of varying the step sizes from those values is shown in Fig. 2. A bidisperse spray of hexane fuel with initial droplet diameters of 50 and 100 μm is considered. The base grid corresponds to $\Delta X = 0.025$ cm and $\Delta t = 2.5$ μs. As ΔX is doubled, the results indicate the presence of numerical diffusion that increases the speed of flame propagation as demonstrated by the larger pressure values. The presence of numerical diffusion for $\Delta X = 0.5$ cm is also evident in Fig. 3 where the gas temperature profiles are shown for the two grid sizes. As seen there, the flame propagates faster as a result of greater numerical diffusion when ΔX is doubled (in Fig. 3b). Note that a hybrid upwind/central discretization scheme has been employed for the convective term of the gas-phase equations. Although it is not shown here, as ΔX is reduced from 0.025 cm, the changes were found to be insignificant. The increase of Δt from 2.5 μs to 5 μs, as indicated in Fig. 2, also has only a small effect on the pressure vs time plot. Thus, the values of $\Delta X = 0.025$ cm and $\Delta t = 5$ μs yield sufficiently accurate results and are employed for all the computations reported here. The validity of the finite-difference calculations was also verified by keeping track of the total mixture mass in the constant-volume combustor. The results indicated that it was conserved within a 1% error. It is also noteworthy that the value of $\Delta X = 0.025$ cm is much smaller than the average droplet spacing but much larger than the droplet size. Thus, the phenomenon of interest is resolved over a scale smaller than the average droplet spacing, but larger than the droplet size.

The general characteristics of flame propagation in a polydisperse spray are depicted in Figs. 4–6. For all the results presented here, unless it is specified otherwise, the initial pressure and overall equivalence ratio are both unity. The size distribution corresponds to the discretized Nukiyama-Tanasawa distribution, and the fuel is n-decane. It is interesting to note that the flame characteristics of this polydisperse spray are generally similar (except for the effect of numerical diffusion in the earlier results) to those discussed for a monodisperse spray by Aggarwal and Sirignano.[6] The characteristics that are common in the two cases are the following:

1) The gas temperature profiles at different times indicate a flame propagating to the right. The flame has predominantly a diffusionlike character. In the flame region, characterized by a steep temperature gradient, the local fuel vapor and oxygen concentrations are quite small, indicating very fast kinetics. There is a fuel-rich region behind the flame and an oxygen-rich region ahead of the flame. The oxygen is diffusing toward the flame region from the right, and the fuel vapor is diffusing from the left. All these indicate a typical diffusion flame behavior.

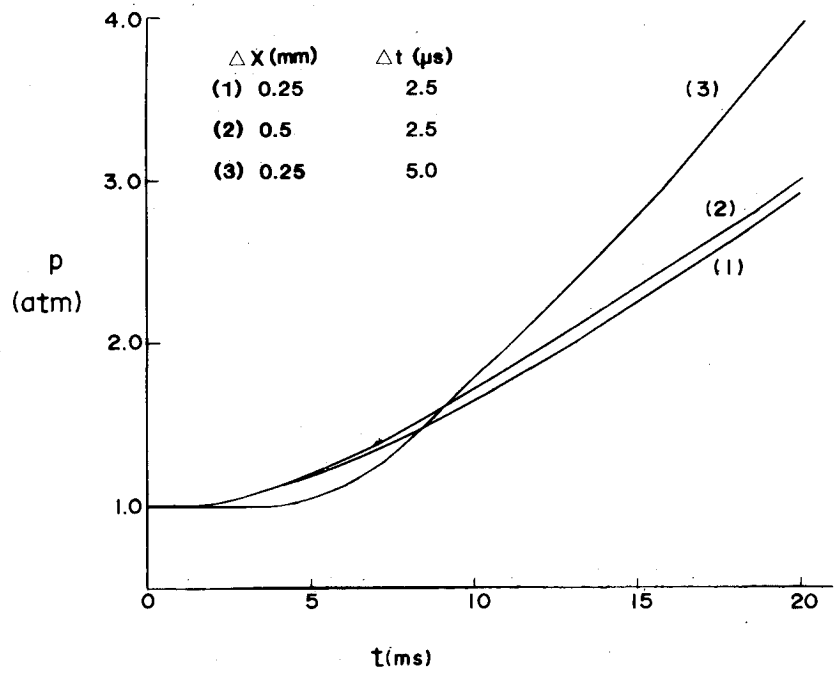

Fig. 2 Pressure vs time plot for three different grids.

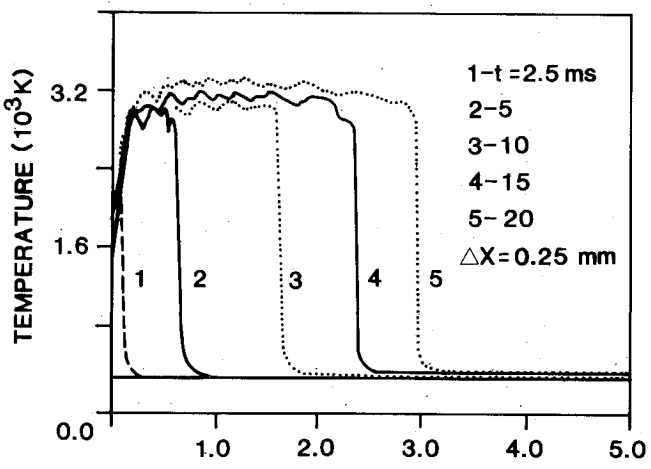

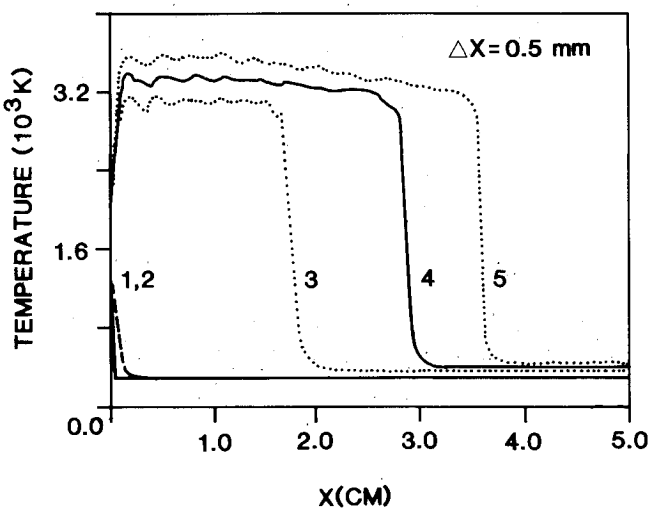

Fig. 3 Gas-temperature profiles at different times for a bidisperse hexane spray.

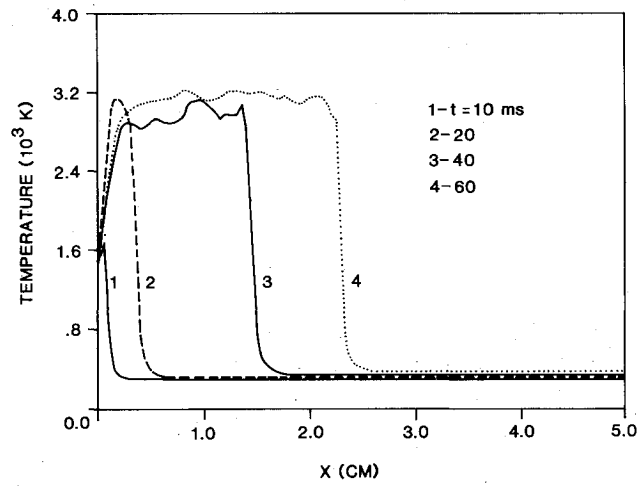

Fig. 4 Gas-temperature profiles at different times for a polydisperse decane spray.

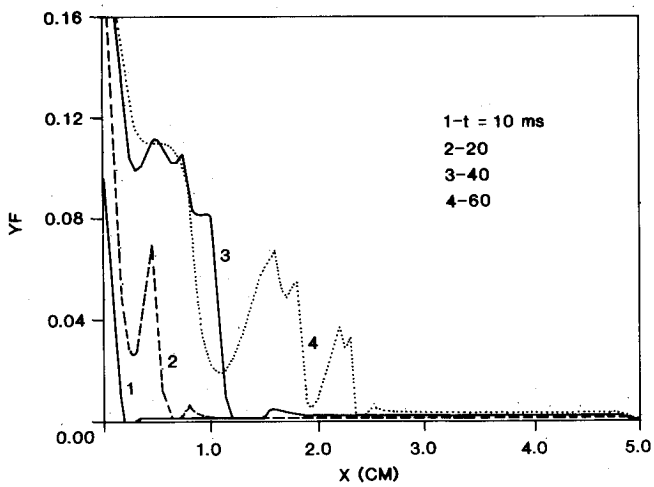

Fig. 5 Fuel vapor mass fraction profiles for the conditions of Fig. 4.

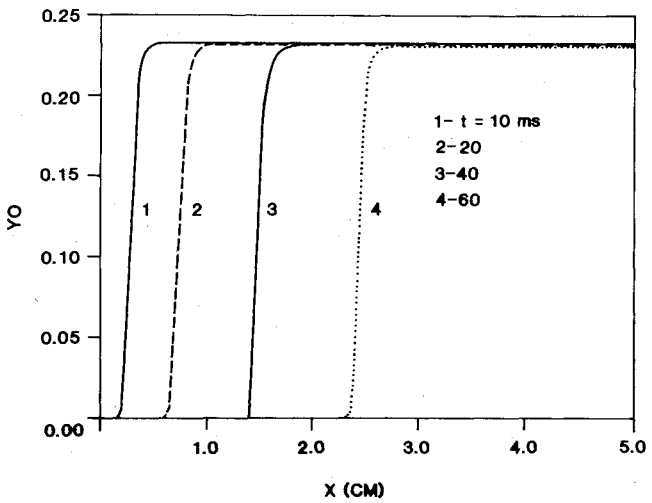

Fig. 6 Oxygen mass fraction profiles for the conditions of Fig. 4.

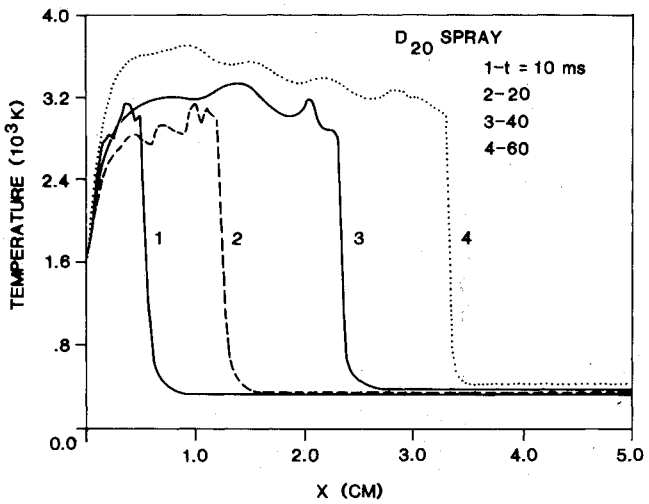

Fig. 7 Gas temperature profiles for the d_{20} spray.

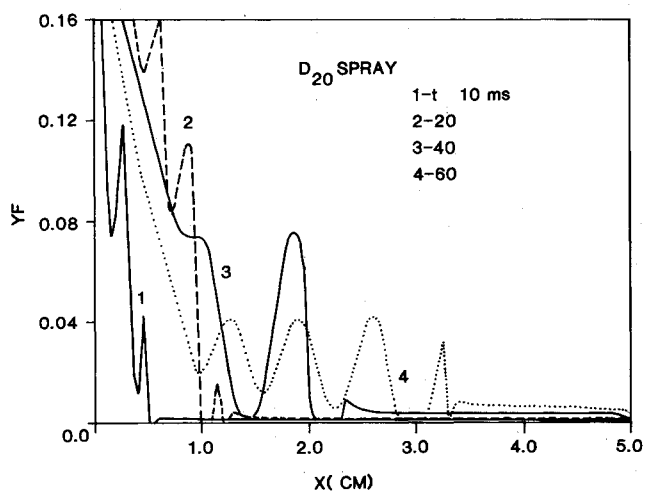

Fig. 8 Fuel vapor mass fraction profiles for the conditions of Fig. 7.

2) At later times, some premixed character is developing. This is due to the droplet vaporization ahead of the flame, which is just sufficient to support a premixed flame. The degree of premixed burning, as compared to the diffusional burning, would depend on the fuel volatility and initial droplet size.

3) The local minima in gas temperature profiles and the corresponding local maxima in fuel vapor mass fractions correspond to instantaneous droplet locations; the vaporizing droplets act as sinks of energy and sources of fuel vapor.

There are also some differences between the two cases. These are the following:

1) The presence of numerical diffusion in the previous results makes the flame propagation faster there.

2) The flame has less premixed character in the present case. It is believed that the numerical diffusion can impart some premixed character to the flame, since with numerical diffusion, the gas temperature ahead of the flame would be higher. This would enhance the vaporization rate, resulting in a higher fuel vapor mass fraction ahead of the flame and thus enhanced premixed character.

3) The local maxima in the fuel vapor mass fraction profiles are less well defined now as compared to the previous results; the distance between two consecutive peaks is almost constant in the previous results. This difference can be attributed to the polydisperse nature of the spray in the present case. The different size droplets move at different speeds that lead to less well-defined spatial distribution of droplets for the polydisperse situation.

It is clear that some of these differences are attributable to the fact that the previous results were affected by numerical diffusion, which, if eliminated, would remove these differences. This indeed is the case, as discussed later.

The similarity between the present polydisperse results and monodisperse results[6] is very interesting and not all that surprising, if we note that the Sauter mean diameter of the polydisperse spray is 103 μm and the droplet diameter of monodisperse spray[6] is 105 μm. Clearly, a strong correlation between the flame characteristics of polydisperse spray and its equivalent d_{32} monodisperse spray is indicated. This aspect is further discussed later.

Let us now examine the correlation between the polydisperse spray and its equivalent d_{20} monodisperse spray. The profiles of gas-phase properties for this monodisperse spray are given in Figs. 7 and 8. Comparisons of these profiles with the corresponding polydisperse case does indicate some qualitative similarities. However, there are significant differences that need to be discussed. First of all, the flame propagation for the d_{20} monodisperse case is much faster than that for the corresponding polydisperse spray. A plausible explanation is that there is relatively more vaporization (ahead of the flame) in the monodisperse case. Although the vaporization is not significantly greater, it appears to enhance the flame propagation noticeably. The effect is more vividly demonstrated if we compare the reaction-rate profiles for the two cases. The reaction-rate profiles, normalized by the maximum reaction-rate values, for the polydisperse and d_{20} monodisperse sprays are shown in Fig. 9. The profiles for the polydisperse case indicate predominantly diffusion-flame characteristics; the region of high reaction rates coincides with the region of low mass fractions of fuel vapor and oxygen. However, for the d_{20} monodisperse case, the reaction-rate profiles indicate a dual burning mechanism; the diffusion-like character as well as the premixed-like character, with the diffusion flame following the premixed-type flame. The amount of premixed-type burning appears to be comparable to the diffusion-type burning and, thus, causes a significant increase in the rate of flame propagation for the monodisperse case.

As mentioned earlier, a global comparison of the polydisperse spray flame with the corresponding d_{32} and d_{20} monodisperse spray flame can be best presented in terms of the pressure vs time plots. In Fig. 10, this comparison is shown for two different cases. The fuel is n-decane and the Nukiyama-Tanasawa distribution is used for the polydisperse sprays. For case 1, the initial droplet diameters for the polydisperse spray are 42, 100, 160, and 200 μm, whereas for

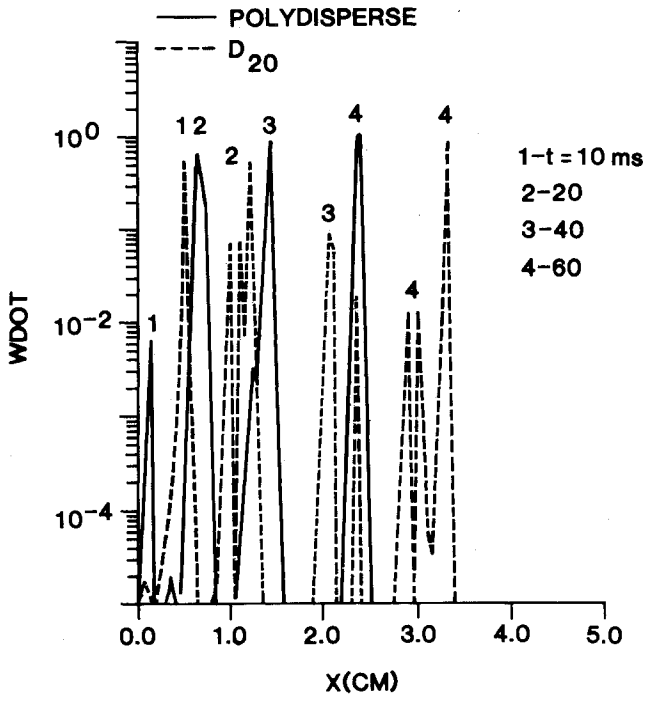

Fig. 9 Reaction-rate profiles for polydisperse and d_{20} monodisperse sprays.

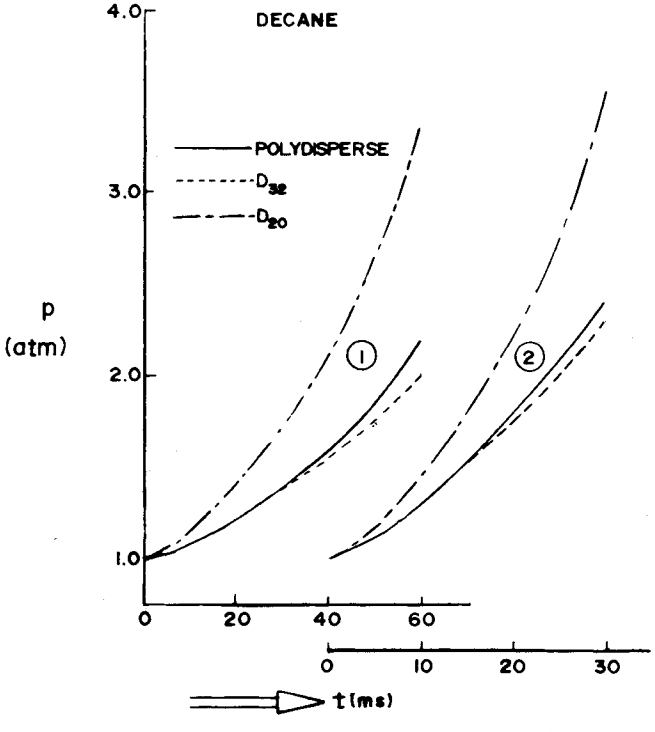

Fig. 10 Pressure vs time for the polydisperse and equivalent d_{32} and d_{20} sprays.

case 2, the values are 20, 48, 76, and 103 μm. The Sauter mean diameters for these cases are 103 and 51 μm, respectively. The corresponding surface-area mean diameters are 72 and 35 μm. The comparison again substantiates the arguments just presented, i.e., the flame characteristics of a polydisperse spray are best correlated by its equivalent d_{32} monodisperse spray and rather poorly by the corresponding d_{20} spray.

Several additional results are now presented to examine the degree of correlation between the polydisperse and corresponding d_{32} and d_{20} monodisperse sprays over a range of parameters. The important parameters are fuel volatility, initial droplet size, overall equivalence ratio, and droplet size distribution. The results for several of these parameters are summarized in Fig. 11. The first two sets are for bidisperse hexane sprays with initial droplet diameters of 50 and 100 μm for the first set and 80 and 160 μm for the second set. The corresponding d_{32} and d_{20} values are 66 and 57 μm for the first set, and 106 and 92 μm for the second set. The third and fourth sets are for the Nukiyama-Tanasawa distribution with initial diameters of 20, 48, 76, and 103 μm, with $d_{32} = 51$ μm and $d_{20} = 35$ μm. The overall equivalence ratio is unity for the first three sets and is 0.65 for the fourth one. For each case, the pressure vs time plot is given for the polydisperse spray and its equivalent d_{32} and d_{20} monodisperse sprays. For all these cases, it is quite evident that the flame chacteristics of polydisperse sprays are best correlated by the Sauter mean diameter and not by the surface-area mean diameter. For the monodisperse spray represented by d_{20}, the flame propagation is much faster than for the corresponding polydisperse spray. As discussed earlier, this is attributable to the fact that the d_{20} spray exhibits more of a premixed-typed flame character due to the enhanced droplet vaporization ahead of the flame. This additional premixed-type burning augments the diffusion-type burning that otherwise exists.

The major conclusion that emerges from the foregoing discussion is that the flame characteristics of polydisperse sprays can be reasonably represented by the equivalent d_{32} monodisperse sprays. On the other hand, they are rather poorly represented by the d_{20} sprays, since quantitative as well as qualitative differences are observed. These results are in complete contrast to those for the ignition behavior,[3] in which the d_{20} sprays provided the best correlation to the polydisperse sprays. This is quite interesting and warrants further examination, as discussed in the next section.

Spray Ignition Characteristics

The study of Aggarwal and Sirignano[3] employed a bidisperse spray and established that the ignition characteristics of polydisperse sprays are best correlated to those of d_{20} monodisperse sprays and not of d_{32} sprays. Since the Nukiyama-Tanasawa distribution was not considered in that study, the ignition results are now presented for this distribution. The normalized ignition delay times vs the overall equivalence ratio are shown in Figs. 12 and 13. For Fig. 12, the fuel is n-decane and the initial droplet diameters are 42, 100, 160, and 200 μm with d_{32} and d_{20} being 103 and 73 μm, respectively. The results in Fig. 13 are for n-hexane with initial diameters of 20, 48, 76, and 103 μm with d_{32} and d_{20} being 51 and 35 μm, respectively. The results confirm the conclusions of the earlier study[3] that the ignition behavior of polydisperse sprays is better correlated by the surface-area mean diameter as compared to the Sauter mean diameter. The correlation between polydisperse and d_{20} sprays is excellent for large droplet size and/or less volatile fuel, as indicated in Fig. 12. On the other hand, the Sauter mean diameter provides a poor approximation for the ignition behavior of polydisperse sprays. Note that the ignition process is more vaporization-controlled in this case. As the ignition process becomes kinetically controlled, which occurs at small droplet sizes and for volatile fuels as in Fig. 13, the correlation between polydisperse and d_{20} sprays is then not quite as good as in the preceding case, although d_{20} still approximates the polydisperse spray behavior better than d_{32}. It is further notable that as the ignition process is made more kinetically controlled, it becomes less sensitive to the initial size distribution, and consequently, the

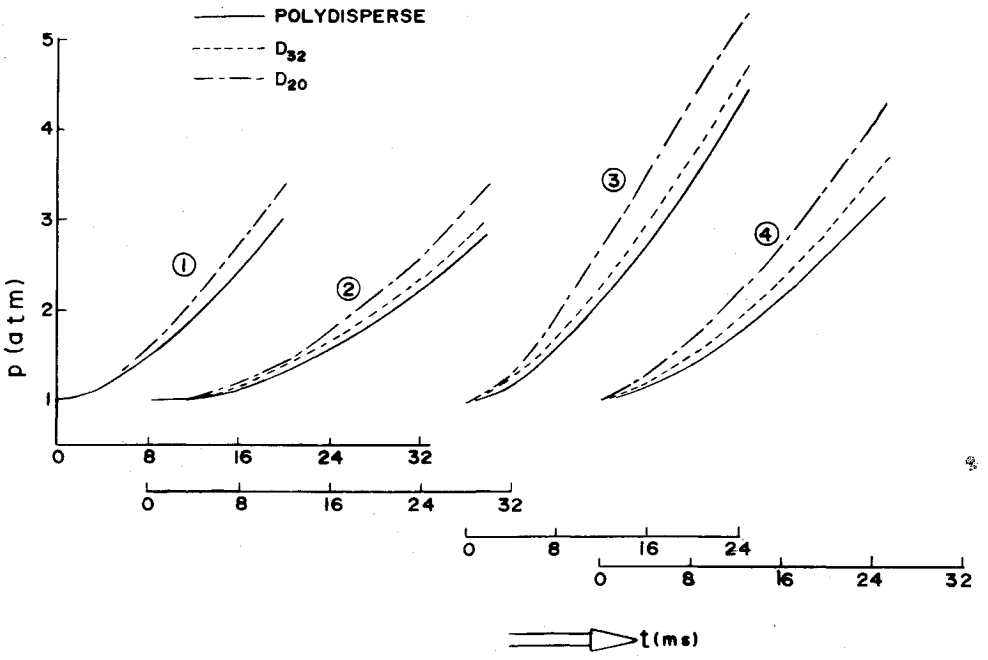

Fig. 11 Pressure vs time for n-hexane spray with bidisperse and Nukiyama-Tanasawa distributions.

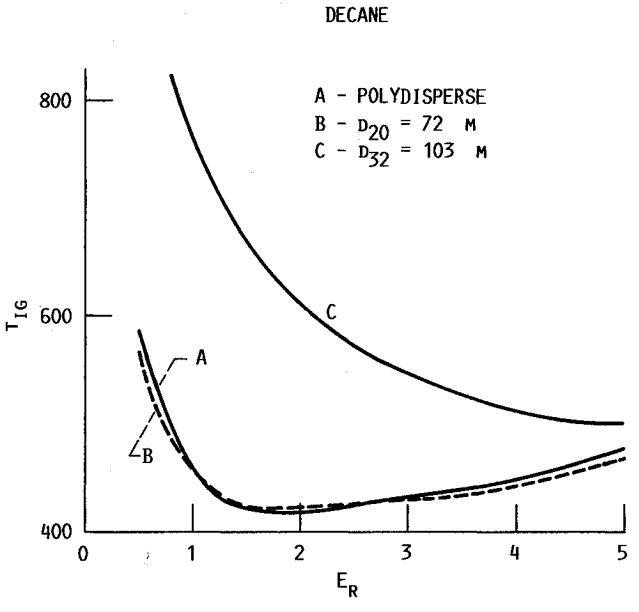

Fig. 12 Normalized ignition delay time vs equivalence ratio. Normalization time = 5 μs.

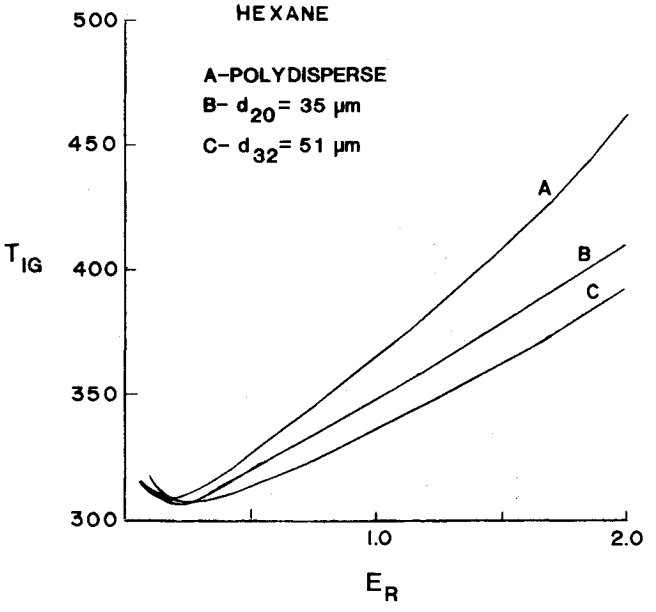

Fig. 13 Normalized ignition delay time vs equivalence ration.

distinction between polydisperse and equivalent monodisperse sprays becomes less clear. This is quite evident in Fig. 13. As the equivalence ratio is reduced, which makes the ignition behavior more kinetically controlled, the difference in ignition delay times as predicted by the polydisperse, d_{32} and d_{20} sprays becomes less significant. This aspect is further discussed in the earlier study.[3]

The important observation, when the ignition results are compared with those on flame propagation, is that the ignition behavior of the polydisperse sprays is best represented by the surface-area mean diameter, whereas the flame characteristics are best represented by the Sauter mean diameter. This means that the total spray surface area is an important parameter for the ignition study, whereas for the combustion behavior, both the total spray volume as well as spray area are important.

Conclusions

The ignition and flame characteristics of polydisperse sprays confined in a constant volume combustor have been numerically studied and compared with those of the corresponding monodisperse sprays represented by the Sauter mean diameter and the surface-area mean diameter, respectively. The polydisperse nature of spray has been represented by the Nukiyama-Tanasawa distribution[5] as well as by a bidisperse distribution. The general conclusions are as follows:

1) For both distributions, it is seen that the local as well as global spray characteristics of polydisperse sprays are best correlated to the Sauter mean diameter. The correlation is observed over a range of key parameters, such as fuel volatility, initial droplet size, and overall equivalence ratio. The global comparison is presented in terms of the pressure vs time plots. The local comparison is in terms of the profiles of gas temperature and fuel vapor mass fraction.

2) For the polydisperse sprays, the flame generally has a dual character: diffusion as well as premixed-type. For most situations considered here, it is predominantly diffusion-type due to insufficient vaporization ahead of the flame and due to the fact that a significant amount of liquid fuel is left behind the propagating flame. A d_{20} monodisperse spray enhances the premixed-type character of the flame and consequently predicts a faster flame propagation as compared to the corresponding polydisperse sprays.

3) The fact that the flame characteristic of polydisperse sprays can be represented by the corresponding d_{32} sprays is quite encouraging. Alkidas[2] had concluded that the vaporization behavior of a polydisperse spray can be well represented by the equivalent d_{32} spray. The present results indicate that the combustion behavior can also be adequately simulated by using the Sauter mean diameter. The use of such diameter could circumvent the problem of measuring the detailed size distribution and/or reduce the computational efforts associated with the modeling of realistic polydisperse sprays.

4) The flame propagation results are in complete contrast with those of the ignition study, in which the surface-area mean diameter provides a better correlation to the polydisperse behavior. This means that the total surface area is the key parameter for the spary ignition study, whereas the total spray volume as well as surface area are important parameters for the flame propagation study.

5) The conclusions presented here regarding the concept of using monodisperse sprays to simulate polydisperse spray behavior need verification from experiments or detailed multidimensional numerical studies. The author is pursuing efforts in these directions. For example, recently, the foregoing concept was examined for turbulent evaporating sprays, and some encouraging results were obtained.[13]

Appendix

For a one-dimensional, constant-volume enclosure, the conservation of mass can be written as

$$M_T = \int_0^L \rho \mathrm{d}x$$

Here, M_T equals the total mixture mass in the enclosure, ρ the density, and L the length of the enclosure. Using the equation of state and assuming that the pressure in the enclosure is uniform spatially (a reasonable assumption for low-speed combusting situations such as considered here), we can obtain

$$p = M_T R \left[\int_0^L \left(\frac{1}{T} \right) \mathrm{d}x \right]^{-1} \Big/ W$$

where R is the universal gas constant, W the molecular weight of mixture, and T the gas temperature. This equation is used to calculate the pressure in the enclosure as a function of time. Note that as the processes of ignition and flame propagation occur, the value of the integral decreases and p increases with time. As a result, the pressure vs time plot is a good indicator of the extent of burning that has occurred in the constant-volume combustor.

References

[1]Dickinson, D.R. and Marshall, W.R., "The Rates of Evaporation of Sprays," *AIChE Journal,* Vol. 14, July 1968, pp. 541-552.

[2]Alkidas, A.C., "The Influence of Size-Distribution Parameters on the Evaporation of Polydisperse Dilute Sprays," *International Journal of Heat and Mass Transfer*, Vol. 24, Dec. 1981, pp. 1913-1923.

[3]Aggarwal, S.K. and Sirignano, W.A., "Ignition of Polydisperse Spray; Importance of D_{20}," *Combustion Science and Technology,* Vol. 46, June 1986, pp. 289-300.

[4]Godsave, G.A.E., "Studies of the Combustion of Drops in a Fuel Spray—The Burning of Single Drops of Fuel," 4th International Symposium on Combustion, The Combustion Institute, Pittsburg, PA, 1983, pp. 818-828.

[5]Nukiyama, S. and Tanasawa, Y., "An Experiment on the Atomization of Liquid (5th Report, the Atomization Pattern of Liquids by Means of Air Stream)," *Transactions of Society of Mechanical Engineers of Japan,* Vol. 6(22), 1940, pp. 5-7.

[6]Aggarwal, S.K. and Sirignano, W.A., "Unsteady Spray Flame Propagation in a Closed Volume," *Combustion and Flame,* Vol. 62, Oct. 1985, pp. 69-84.

[7]Seth, B., Aggarwal, S.K., and Sirignano, W.A., "Flame Propagation Through an Air-Fuel Spray Mixture with Transient Vaporization," *Combustion and Flame,* Vol. 39, Oct. 1980, pp. 149-168.

[8]Aggarwal, S.K., "Chemical-Kinetics Modeling for the Ignition of Idealized Sprays," *Combustion and Flame*, Vol. 69, Sept. 1987, pp. 291-302.

[9]Williams, F.A., "Progress in Spray-Combustion Analysis," 8th International Symposium on Combustion, The Combustion Institute, Pittsburgh, PA, 1963, pp. 50-69.

[10]Rosin, P. and Rammler, E., "Laws Governing the Fineness of Powdered Coal," *Journal of Institute of Fuel,* Vol. 7, 1933, pp. 29-36.

[11]Tishkoff, J.M. and Law, C.K., "Application of a Class of Distribution Functions to Drop-Size Data by Logarithmic Least Square Technique," *Engineering for Power,* Vol. 99, Oct. 1977, pp. 684-688.

[12]Hiroyasu, H. and Kadota, T., "Fuel Droplet Size Distribution in Diesel Combustion Chamber," SAE Paepr 740715, 1974.

[13]Aggarwal, S.K. and Shuen, S.J.," Representation of the Vaporization Behavior of Turbulent Polydisperse Sprays by Equivalent Monodisperse Sprays," AIAA Paper 87-1954, June 1987.